Performance evaluation of combined adsorption refrigeration cycles

Khairul Habib [a], Bidyut Baran Saha [b,*], Anutosh Chakraborty [c], Shigeru Koyama [d], Kandadai Srinivasan [e]

[a] Solar Energy Research Institute of Singapore, National University of Singapore, 7 Engineering Drive 1, Block E3A, #06-01, Singapore 117574, Singapore
[b] Mechanical Engineering Department, Kyushu University, 744 Motooka, Nishi-ku, Fukuoka 819-0395, Japan
[c] School of Mechanical and Aerospace Engineering, Nanyang Technological University, 50 Nanyang Avenue, Singapore 639798, Singapore
[d] Interdisciplinary Graduate School of Engineering Sciences, Kyushu University, 6-1 Kasuga-koen, Kasuga, Fukuoka 816-8580, Japan
[e] Mechanical Engineering Department, National University of Singapore, 9 Engineering Drive 1, Singapore 117575, Singapore

ARTICLE INFO

ABSTRACT

This paper presents the results of an investigation on the performance of combined adsorption refrigeration cycles. The novel combined cycle amalgamates the activated carbon (AC)-R507A as the bottoming cycle and AC-R134a cycle as the topping cycle and deliver refrigeration load at as low as $-10\,°C$ at the bottoming cycle. The cycle simulation is based on the experimentally confirmed adsorption isotherms, kinetics and isosteric heat of adsorption data for R134a and R507A on highly porous based activated carbon of type Maxsorb III. The optimum cooling capacity, coefficient of performance (COP) and chiller efficiency are calculated in terms of cycle time, switching time, regeneration and brine inlet temperatures. Results show that the combined adsorption cycles are feasible even when low-temperature heat source is available.

Evaluation de la performance des cycles frigorifiques combinés à adsorption

* Corresponding author. Tel.: +81 92 802 3101; fax: +81 92 802 3125.
  E-mail address: saha@mech.kyushu-u.ac.jp (B.B. Saha).

Nomenclature

Symbols

A	area, m^2
COP	coefficient of performance, –
C_p	specific heat capacity, $J\,kg^{-1}\,K^{-1}$
D_s	surface diffusion coefficient, $m^2\,s^{-1}$
D_{so}	pre-exponential constant, $m^2\,s^{-1}$
E_a	activation energy, $J\,kg^{-1}$
h	enthalpy, $J\,kg^{-1}$
m	mass, kg
$\dot{m}$	mass flow rate, $kg\,s^{-1}$
P	pressure, Pa
P_s	saturation pressure, Pa
Q	power, W
R	gas constant, $J\,kg^{-1}\,K^{-1}$
R_p	adsorbent radius, m
T	temperature, K
t_{cycle}	cycle time, s
t	time, s
U	overall heat transfer coefficient, $W\,m^{-2}\,K^{-1}$
W	volumetric uptake, $m^3\,kg^{-1}$
W_0	limiting volumetric uptake, $m^3\,kg^{-1}$
E	characteristic energy, $J\,kg^{-1}$
n	heterogeneity constant, –
x	instantaneous uptake, $kg\,kg^{-1}$
x^*	equilibrium uptake, $kg\,kg^{-1}$
x_0	limiting adsorption uptake, $kg\,kg^{-1}$
Q_{st}	isosteric heat of adsorption, $J\,kg^{-1}$
η	chiller efficiency, –

Subscripts

ac	activated carbon
al	aluminum
cu	copper
f	liquid phase
g	gaseous phase
in	inlet
out	outlet
w	water
ads	adsorber
bed	sorption heat exchanger (adsorber/desorber)
cond	condenser
eva	evaporator
des	desorber
brine	brine
h	hot water

Superscripts

R134a	1,1,1,2-tetrafluoroethane
R507A	an equal mass fraction azeotropic blend of R125 and R143a

1. Introduction

During the last two decades, study on thermally powered adsorption refrigeration system has gained considerable interest due to its ability to combat ozone depletion problem which was caused by the utilization of CFCs and HCFCs in cooling systems (Meunier, 1998). The adsorption cooling and refrigeration systems have the advantages of being (i) compact, (ii) free or nearly free of moving parts (iii) efficiently driven by low-temperature waste heat or renewable energy sources, and (iv) free of toxic and environmentally-harmful substances as these systems can use natural refrigerants such as water (Saha et al., 2003), ethanol (El-Sharkawy et al., 2006), methanol (Wang et al., 1997), ammonia (Miles and Shelton, 1996), etc. and (v) do not require any synthetic lubricants such as polyolesters. Thermally powered adsorption cooling cycle could be operated below or above atmospheric pressures. Examples of adsorbent–refrigerant pairs working at sub-atmospheric conditions are silica gel–water (Chua et al., 2004; Saha et al., 2001, 2006), zeolite–water (Lai, 2000; Wang et al., 2006; Zhang, 2000), activated carbon fiber––ethanol (Saha et al., 2007a,b), activated carbon–methanol (Anyanwu and Ezekwe, 2003; Pons and Guilleminot, 1986) pairs. In order to employ adsorption cycles for refrigeration applications, cascading schemes have been introduced (Alam, 2000). Table 1 lists the combined adsorption cycles employing various adsorbent–refrigerant pairs for cooling application.

Adsorption as standalone system for refrigeration application has the disadvantage of poor system performances in terms of both specific cooling capacity and COP. When refrigeration is a part of a process industry, where considerable amount of waste heat is available or where low grade solar thermal energy is available, the combination of two adsorption systems could be advantageous.

From the above perspective, this study presents the performance investigation results of combined adsorption refrigeration cycles which amalgamate two adsorption cycles namely AC-R134a and AC-R507A such that the cooling loads at temperature as low as −10 °C can be met at the evaporator of the high vapor pressure (in this case R507A) bottoming cycle. A cycle simulation computer program of the novel combined adsorption refrigeration systems is developed to analyze the cooling capacity, COP and chiller efficiency variations by varying adsorption/desorption cycle times, switching times, size of adsorbent beds, regeneration and brine inlet temperatures.

2. Working principle of combined cycles

Each of the upper stage (operating on R134a) and the lower stage (operating on R507A) of the combined cycle comprises an evaporator, a condenser and two sorption elements (SEs). A schematic diagram of the combined cycle is shown in the Fig. 1 where a integraded heat exchanger combining the roles

Table 1 – Combined adsorption cycles for cooling application.			
Adsorbent–refrigerant pair	System description	Adsorption characteristics and performance	Sources
Zeolite + water, Silica gel + water	Two zeolite–water and one silica gel–water systems. Zeolite–water pair in the topping stage while silica gel–water pair in the bottoming stage.	Adsorption isotherms: Langmuir model for Zeolite –water pair Freundlich model for silica gel–water pair COP: 1.35 when $T_h = 230\,°C$ Specific cooling power: 42.7 W/kg	Liu and Leong, 2006
Zeolite + water, Active carbon + methanol	Two zeolite–water pairs in the topping cycle while silica gel–water pair in the bottoming cycle.	Adsorption isotherms: Not mentioned COP: 1.06 $T_h = 220\,°C$, $T_{eva} = 25\,°C$, $T_{cond} = 35\,°C$	Douss and Meunier, 1989
Zeolite + water, Active carbon + methanol	Low-temperature activate carbon + methanol cycle boosted by a high temperature double effect zeolite –water cycle	Heat source temperature of zeolite–water system is 275 °C. Refrigeration load of −10 °C with a COP of 0.85	Meunier, 1986
Zeolite-13X + water SWS-2L + water	Zeolite–water for topping stage while SWS-2L + water for bottoming stage	Adsorption isotherms: Not mentioned COP: 0.275 for zeolite + water system, $T_{eva} = -10\,°C$, $T_{cond} = 55\,°C$, $T_{ads} = 38°$, $T_h = 292\,°C$	Dawoud, 2007
Silica gel + water incorporated with mechanical booster pump	Suction pump-assisted thermal and electrical hybrid adsorption heat pump	Adsorption isotherms: Not mentioned Performance improved 1.6 times as that of a thermally operated heat pump	Hirota et al., 2008
Vapor compression (R-22) system + solar operated absorption (ammonia + water) system	Condenser of R-22 system is cooled by evaporator of ammonia system	Savings in electrical energy consumption by compression system	Chinnappa et al., 1993
Thermal compression (Activated carbon + R134a) + Mechanical compression system	Mechanical compression is supplemented by thermal compression using a string of adsorption compressors	Adsorption isotherms: Dubinin–Astakhov (D–A) for activated carbon/R134a system. 40% energy saving is achieved.	Banker et al., 2008

of the condenser of R507A cycle and the evaporator of R134a cycle is employed. The shell and tube heat exchanger has R134a on the tube side and R507A on the shell side. The cooling load of the combined cycle is met by the AC-R507A segment. The evaporated refrigerant in the R507A cycle is adsorbed onto the adsorbent and stored in the cold bed or the adsorber. Adsorption is an exothermic process, with the adsorber to be cooled by a coolant so as to sustain the adsorption process. As the adsorbent in the cold bed gets saturated, the other bed which is previously regenerated by heating has to take over its role. Desorption is an endothermic process, and a heat source is used at the hot bed to sustain the process. The desorbed vapor is condensed at the integrated condenser and the warm condensate is refluxed back to the evaporator through an expansion valve.

3. Mathematical modeling

3.1. Adsorption isotherms

Dubinin–Astakhov (D–A) model, which is expressed by Eq. (1), is used to estimate the equilibrium uptake of both AC-R134a and AC-R507A pairs

$$W = W_0 \exp\left[-\left\{ \frac{RT}{E} \ln\left(\frac{p_s}{p}\right) \right\}^n \right] \tag{1}$$

The numerical values of W_0, n and E for AC-R507A cycle are evaluated experimentally by Saha et al. (2008), which are found to be 1.17×10^{-3} m³/kg, 1.47 and 58.04 kJ kg⁻¹, respectively. Saha et al. (2009) also measured the adsorption characteristics of AC-R134a pair and obtained the numerical values of W_0, E and n as 1.66×10^{-3} m³ kg⁻¹, 82.9 kJ kg⁻¹ and 1.3, respectively.

3.2. Adsorption kinetics

In the current adsorption chiller model, the rate of adsorption or desorption is governed by the Fickian diffusion model (Habib, 2009).

$$D_s = D_{so} \exp\left(-\frac{E_a}{RT} \right) \tag{2}$$

$$x = x^* \left[1 - \frac{6}{\pi^2} \sum_{n=1}^{\infty} \frac{1}{n^2} \exp\left(-\frac{n^2 \pi^2 D_s t}{R_p^2} \right) \right] \tag{3}$$

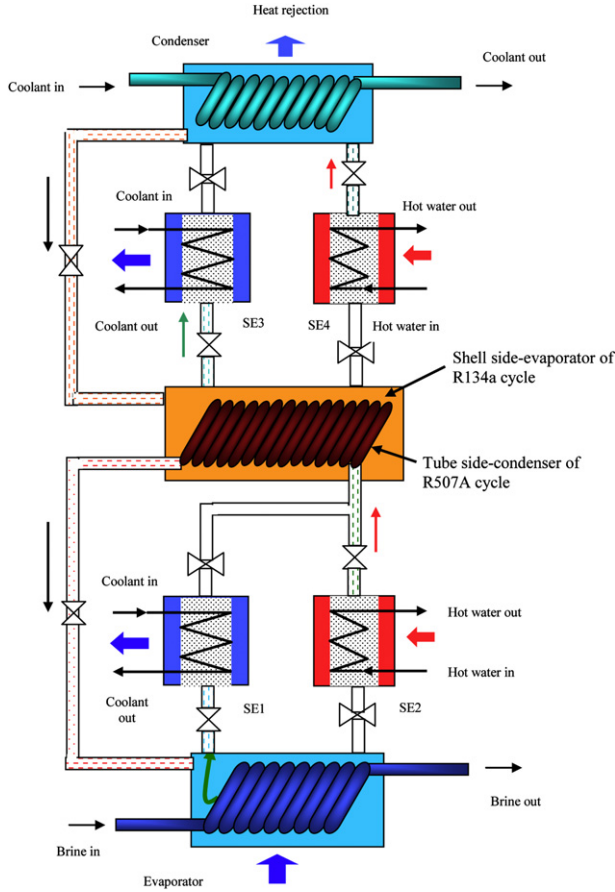The kinetics of AC-R134a and AC-R507A pairs has been

Fig. 1 – Schematic diagram of combined adsorption chiller.

evaluated by constant volume variable pressure (CVVP) method (Habib et al., 2010). Employing the Arrhenius equation, the surface diffusion D_s is calculated and the numerical values of D_{so} and E_a for AC-R134a system are found to be 1.44×10^{-11} m^2/s and 90.49 kJ kg^{-1}, respectively. For AC-R507A cycle, the numerical values of D_{so} and E_a are obtained to be 3.41×10^{-11} m^2 s^{-1} and 119.7 kJ kg^{-1}, respectively.

3.3. Isosteric heat of adsorption

The isosteric heat of adsorption for both AC-R134a and AC-R507A and can be expressed as (El-Sharkawy et al., 2007)

$$Q_{st} = h_{fg} + E\left[\left\{\ln\left(\frac{x_0}{x^*}\right)\right\}^{\frac{1}{n}} + a\left(\frac{T}{T_c}\right)^b\right] \tag{4}$$

For AC-R134a system, the values of a and b are 1.81 and 6.21, respectively. For AC-R507A system, the values of a and b are 2.6 and 6.38, respectively.

3.4. Adsorption and desorption energy balance

3.4.1. AC-R134a cycle
The adsorption bed comprises activated carbon, the adsorber body, the heat exchanger fins and tubes, and the energy balance equation is given by

$$\left[m_{ac}C_{p,ac} + m_{ac}C_p^{R134a}x^{R134a} + m_{Al}C_{p,Al} + m_{Cu}C_{p,Cu}\right]\frac{dT_{ads/des}^{R134a}}{dt}$$
$$= \delta m_{ac}\left\{h_g\left(P_{eva/cond}^{R134a}, T_{ads/des}^{R134a}\right) - h_g\left(T_{eva/cond}^{R134a}\right) + Q_{st}^{R134a}\right\}\frac{dx_{ads/des}^{R134a}}{dt} \tag{5}$$
$$+ \dot{m}_w C_{p,w}\left(T_{w,in,ads/des}^{R134a} - T_{w,out,ads/des}^{R134a}\right)$$

where $\delta = 1$ for adsorption/desorption cycle operation, and during switching, $\delta = 0$. The left hand side of adsorber/desorber energy balance equation (Eq. (5)) indicates the rate of change of internal energy due to the thermal mass of adsorbent(s), the refrigerant (R134a) and adsorber/desorber heat exchanger during adsorption and desorption. The first term on the right hand side of Eq. (5) represents the adsorption heat during adsorption process or the input of desorption heat during desorption process. The second term on the right hand side of Eq. (5) defines the total amount of heat released to the cooling water upon adsorption or provided by the heating source (hot water) for desorption. For a small temperature difference across heating/cooling fluid such as water, the outlet temperature of the source is sufficiently accurate to be modeled by the log mean temperature difference (LMTD) method and it is given by:

$$T_{w,out,bed}^{R134a} = T_{bed}^{R134a} + (T_{w,in,bed}^{R134a} - T_{bed}^{R134a})\exp\left[-\frac{(UA)_{bed}^{R134a}}{(\dot{m}C_p)_w}\right] \tag{6}$$

3.4.2. AC-R507A cycle
The energy balance of adsorber/desorber of AC-R507A cycle can be expressed as,

$$\left[m_{ac}C_{p,ac} + m_{ac}C_p^{R507A}x^{R507A} + m_{Al}C_{p,Al} + m_{Cu}C_{p,Cu}\right]\frac{dT_{ads/des}^{R507A}}{dt}$$
$$= \delta m_{ac}\left\{h_g\left(P_{eva/cond}^{R508A}, T_{ads/des}^{R507A}\right) - h_g\left(T_{eva/cond}^{R507A}\right) + Q_{st}^{R507A}\right\}\frac{dx_{ads/des}^{R507A}}{dt} \tag{7}$$
$$+ \dot{m}_w C_{p,w}\left(T_{w,in,ads/des}^{R507A} - T_{w,out,ads/des}^{R507A}\right)$$

The left hand side of adsorber/desorber energy balance equation Eq. (7) provides the rate of change of internal energy due to the thermal mass of adsorbent(s), the refrigerant (R507A) and adsorber/desorber heat exchanger during adsorption and desorption. The first term on the right hand side of Eq. (7) represents the release of adsorption heat during adsorption process or the input of desorption heat during desorption process. The second term on the right hand side of Eq. (7) defines the total amount of heat released to the cooling water upon adsorption or provided by the hot water for desorption. The temperature of the water outlet from the adsorber/desorber of R507A cycle can be written as,

$$T_{w,out,bed}^{R507A} = T_{bed}^{R507A} + (T_{w,in,bed}^{R507A} - T_{bed}^{R507A})\exp\left[-\frac{(UA)_{bed}^{R507A}}{(\dot{m}C_p)_w}\right] \tag{8}$$

3.5. Evaporator energy balance

3.5.1. AC-R134a cycle
The integrated heat exchanger is the evaporator of R134a cycle and the condenser of R507A cycle. The overall energy balance of the evaporator in the R134a cycle is dominated mainly by the heat interaction between the evaporator and the adsorption bed and the heat transferred from the

condenser of R507A cycle. The heat released from the condenser is also taken into account. The energy balance equation of the evaporator can be expressed as,

$$
\begin{aligned}
\left(m_{eva}^{R134a}C_{p,eva} + m_{hex}C_{p,Cu}\right)\frac{dT_{eva}^{R134a}}{dt} &= -\delta\Big\{h_g\big(P_{cond}^{R507A}, T_{des}^{R507A}\big) \\
-h_g\big(T_{cond}^{R507A}\big) + h_{fg}^{R507A}\Big\}m_{ac}\frac{dx_{des}^{R507A}}{dt} & \\
+\delta\Big\{h_g\big(P_{eva}^{R134a}, T_{ads}^{R134a}\big) - h_g\big(T_{eva}^{R134a}\big) + h_{fg}^{R134a}\Big\}m_{ac}\frac{dx_{ads}^{R134a}}{dt} &
\end{aligned}
\tag{9}
$$

The left hand side of Eq. (9) denotes the change of internal energy due to the sensible heat of liquid refrigerant and the metal of the heat exchanger tubes in the evaporator. On the right hand side, the first term represents heat transferred from the condenser of R507A cycle; the second term gives the latent heat of evaporation where the effect of gaseous phase due to adsorption has been taken into account.

3.5.2. AC-R507A cycle

The energy balance of R507A cycle in the evaporator can be written as,

$$
\begin{aligned}
\left(m_{eva}^{R507A}C_{p,eva} + m_{hex}^{R507A}C_{p,Cu}\right)\frac{dT_{eva}^{R507A}}{dt} &= -\delta\Big\{h_g\big(P_{eva}^{R507A}, T_{ads}^{R507A}\big) \\
-h_g\big(T_{eva}^{R507A}\big) + h_{fg}^{R507A}\Big\}m_{ac}\frac{dx_{ads}^{R507A}}{dt} & + \\
\left(\dot{m}_{brine}C_{p,brine}\right)\left(T_{brine,in} - T_{brine,out}\right) &- \delta m_{ac}C_p^{R507A}T_{cond}^{R507A}\frac{dx_{des}^{R507A}}{dt}
\end{aligned}
\tag{10}
$$

The left hand side of Eq. (10) denotes the change of internal energy due to the sensible heat of liquid refrigerant and the metal of the heat exchanger tubes in the evaporator. On the right hand side, the first term represents latent heat of evaporation for the amount of refrigerant adsorbed; the second term provides the cooling capacity of the evaporator and the last term stands for the amount of refrigerant flushing back to the evaporator from condenser of R507A cycle. Since, refrigeration load of −10 °C will be achieved from the evaporator of R507A cycle, instead of water, brine is used as the working fluid in the heat exchanger of the evaporator of R507A cycle. The brine outlet temperature can be expressed as,

$$
T_{brine,out} = T_{eva}^{R507A} + \left(T_{brine,in} - T_{eva}^{R507A}\right)\exp\left[-\frac{(UA)_{eva}^{R507A}}{(\dot{m}C_p)_{brine}}\right]
\tag{11}
$$

3.6. Condenser energy balance

3.6.1. AC-R134a cycle

The energy balance of the condenser of R134a cycle can be expressed as,

$$
\begin{aligned}
\left(m_{cond}^{R134a}C_{p,cond} + m_{hex}^{R134a}C_{p,Cu}\right)&\frac{dT_{cond}^{R134a}}{dt} \\
= -\delta\Big\{h_g\big(P_{cond}^{R134a}, T_{des}^{R134a}\big) &- h_g\big(T_{cond}^{R134a}\big) + h_{fg}^{R134a}\Big\}m_{ac}\frac{dx_{des}^{R134a}}{dt} \\
+ \dot{m}_w C_{p,w}&\left(T_{w,in,cond}^{R134a} - T_{w,out,cond}^{R134a}\right)
\end{aligned}
\tag{12}
$$

The left hand side of Eq. (12) defines the rate of change of internal energy of the metallic tubes of the heat exchanger. On the right hand side, the first term represents heat generation

due to condensation where the effects of gaseous phase due to desorption have been taken into account. The last term shows the total amount of heat released to the cooling water. The outlet temperature of the condenser can be expressed using the log mean temperature difference approach,

$$
T_{w,out,cond}^{R134a} = T_{cond}^{R134a} + \left(T_{w,in,cond}^{R134a} - T_{cond}^{R134a}\right)\exp\left[-\frac{(UA)_{cond}^{R134a}}{(\dot{m}C_p)_w}\right]
\tag{13}
$$

3.6.2. AC-R507A cycle

The energy balance of condenser R507A cycle can be expressed as,

$$
\begin{aligned}
\left(m_{cond}^{R507A}C_p^{R507A} + m_{hex}^{R507A}C_{p,Cu}\right)\frac{dT_{cond}^{R507A}}{dt} &= -\delta\Big\{h_g\big(P_{cond}^{R507A}, T_{des}^{R507A}\big) \\
-h_g\big(T_{cond}^{R507A}\big) + h_{fg}^{R507A}\Big\}m_{ac}\frac{dx_{des}^{R507A}}{dt} & + \\
\delta\Big\{h_g\big(P_{eva}^{R134a}, T_{ads}^{R134a}\big) - h_g\big(T_{eva}^{R134a}\big) + h_{fg}^{R134a}\Big\}m_{ac}\frac{dx_{ads}^{R134a}}{dt} &
\end{aligned}
\tag{14}
$$

The left hand side of Eq. (14) defines the rate of change of internal energy of the metallic tubes of the heat exchanger of the condenser of R507A cycle. On the right hand side, the first term represents latent heat of vaporization due to the amount of refrigerant desorbed; the second term gives the latent heat of evaporation where the effect of gaseous phase due to adsorption has been taken into account.

The cooling capacity, Q_{eva}^{cycle} of this combined cycle is achieved at the evaporator of R507A cycle and can be defined as,

$$
Q_{eva}^{cycle} = \frac{1}{t_{cycle}}\int_0^{t_{cycle}} (\dot{m}C_p)_{brine}\left(T_{brine,in} - T_{brine,out}\right)dt
\tag{15}
$$

The driving heat source of R134a and R507A cycles can be written, respectively as,

$$
Q_H^{R134a} = \frac{1}{t_{cycle}}\int_0^{t_{cycle}} (\dot{m}C_p)_{des}\left(T_{h,in} - T_{h,out}\right)dt\bigg|_{R134a}
\tag{16}
$$

$$
Q_H^{R507A} = \frac{1}{t_{cycle}}\int_0^{t_{cycle}} (\dot{m}C_p)_{des}\left(T_{h,in} - T_{h,out}\right)dt\bigg|_{R507A}
\tag{17}
$$

Here t_{cycle} denotes total cycle time.

The overall COP of the combined cycle can be calculated as,
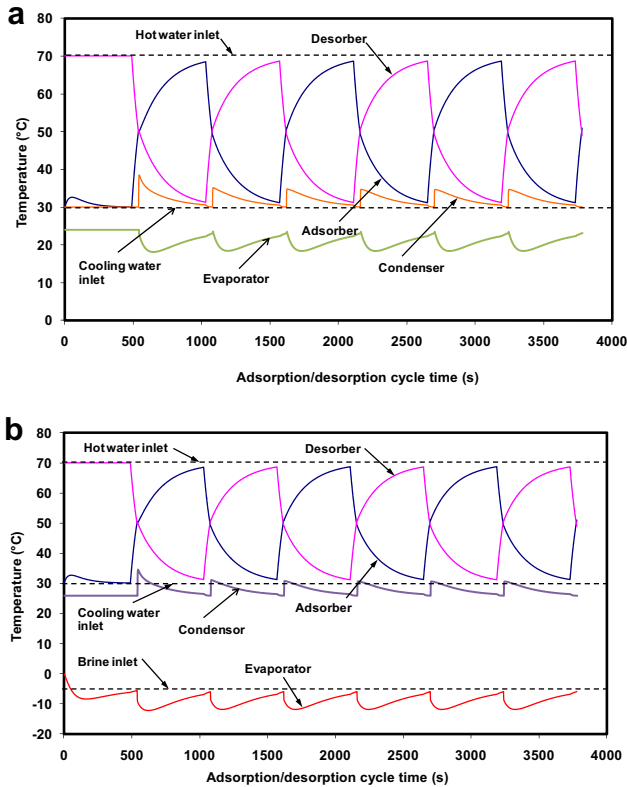
$$
COP = \frac{Q_{eva}^{cycle}}{Q_H^{R134a} + Q_H^{R507A}}
\tag{18}
$$

Chiller efficiency, η of the combined cycle can be expressed as (Saha, 1997),

$$
\eta = \frac{COP}{COP_{CARNOT}}
\tag{19}
$$

where COP_{CARNOT} can be written as,

$$
COP_{CARNOT} = \left(\frac{\overline{T}_{des} - \overline{T}_{cond}}{\overline{T}_{des}}\right)\left(\frac{\overline{T}_{eva}}{\overline{T}_{ads} - \overline{T}_{eva}}\right)
\tag{20}
$$

where, $\overline{T}_{des}$, $\overline{T}_{cond}$, $\overline{T}_{ads}$ and $\overline{T}_{eva}$ indicate the average temperatures of the desorber, condenser, adsorber and evaporator, respectively for one cycle.

Fig. 2 – (a) Temperature profiles for different components of the R134a cycle of the combined adsorption cycle for rated conditions. (b) Temperature profiles for different components of the R507A cycle of the combined adsorption cycle for rated conditions.

Table 3 – Values adopted for simulation.

Symbols	Value	Unit
m_{ac}	50	kg
UA_{bed}	3500	W K^{-1}
UA_{eva}	4770	W K^{-1}
UA_{cond}	15,300	W K^{-1}
m_{cond}	25	kg
m_{eva}	13	kg
$C_{p,ac}$	930	J kg^{-1} K^{-1}
$C_{p,Al}$	904	J kg^{-1} K^{-1}
$C_{p,Cu}$	386	J kg^{-1} K^{-1}

cycle. It can be observed from Fig. 2a that the R134a cycle is able to reach from transient to nearly steady state within three half cycles or 1900 s, while R507A cycle is able to reach from transient to nearly steady state within three half cycles or 1800 s (Fig. 2b).
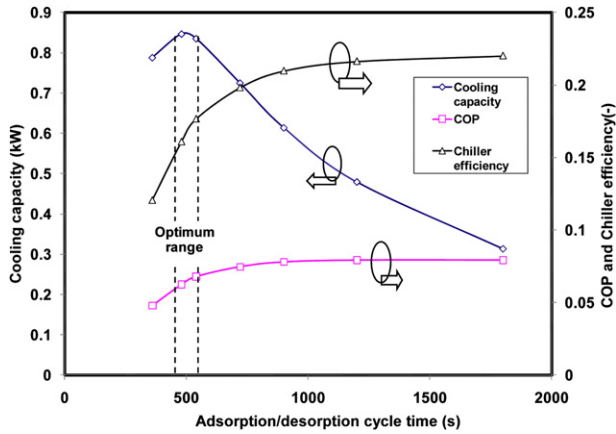
4.2. Adsorption/desorption cycle time

The simulated results of cooling capacity, COP and chiller efficiency variations with adsorption/desorption cycle for the standard heat transfer fluid temperatures and flow rates conditions are shown in Fig. 3. The switching (pre-heating or pre-cooling) time is chosen as 50 s. From Fig. 3, it is observed that the highest cooling capacity for the combined cycle achieved in the evaporator of the bottoming cycle is around 0.85 kW for cycle times between 480 and 520 s. As can be seen from Fig. 3, when the cycle time is shorter than 400 s, it is not sufficient for adsorption or desorption satisfactorily. As a result, cooling capacity decreases abruptly. On the other hand, when cycle time is longer than 720 s, the cooling capacity decreases gradually due to the less intense of adsorption after the first 10 min as the adsorbent reaches toward equilibrium. It can be seen from Fig. 3 that both COP and chiller efficiency increase uniformly for both arrangements with longer adsorption/desorption cycle time. However, after around 900 s, the increase in COP and chiller efficiency values becomes marginal. The optimum values of COP and chiller efficiency are around 0.06 and 0.16, respectively when the adsorption/desorption cycle time is between 500 and 540 s.

4.3. Switching time

The switching time has always been an integral part of adsorption chiller operation. The effects of switching time on

4. Results and discussion

4.1. Chiller transient response

Fig. 2a and b shows the chiller temporal histories for the reactor beds (adsorber/desorber heat exchangers), and heat transfer fluids. Table 2 depicts the rated conditions of both R134a and R507A cycles. The values of the symbols used in the present simulation model are furnished in Table 3. The hot water inlet temperature for both R134a and R507A cycles is taken as 70 °C, while the cooling water inlet temperature for both R134a and R507A cycles is taken as 30 °C. The brine inlet temperature is taken as −5 °C for the evaporator of the R507A

Table 2 – Rated conditions.

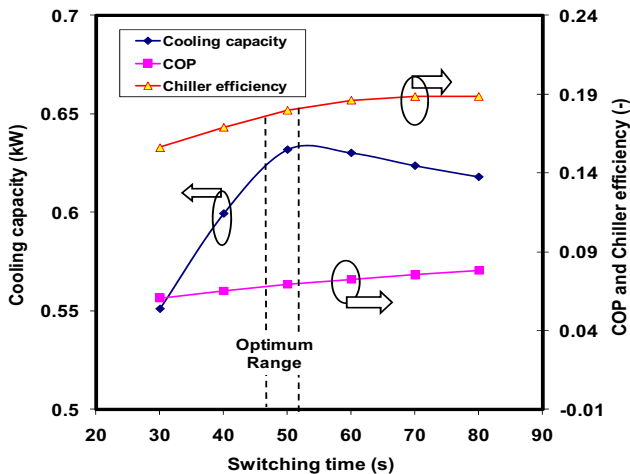| Combined Cycle	Hot water inlet		Cooling water inlet		Brine inlet	
	Temperature (°C)	Flow rate (kg/s)	Temperature (°C)	Flow rate (kg/s) (ads + cond)	Temperature (°C)	Flow rate (kg/s)
R134a cycle	70	0.3	30	(0.3 + 0.3)	−	−
R507A cycle	70	0.3	30	(0.3 + 0.3)	−5	0.1
Adsorption/desorption cycle time for both cycles: 540 s			Switching time for both cycles: 50 s			

Fig. 3 − Adsorption/desorption cycle time effect on cooling capacity, COP and chiller efficiency for combined adsorption cycle.
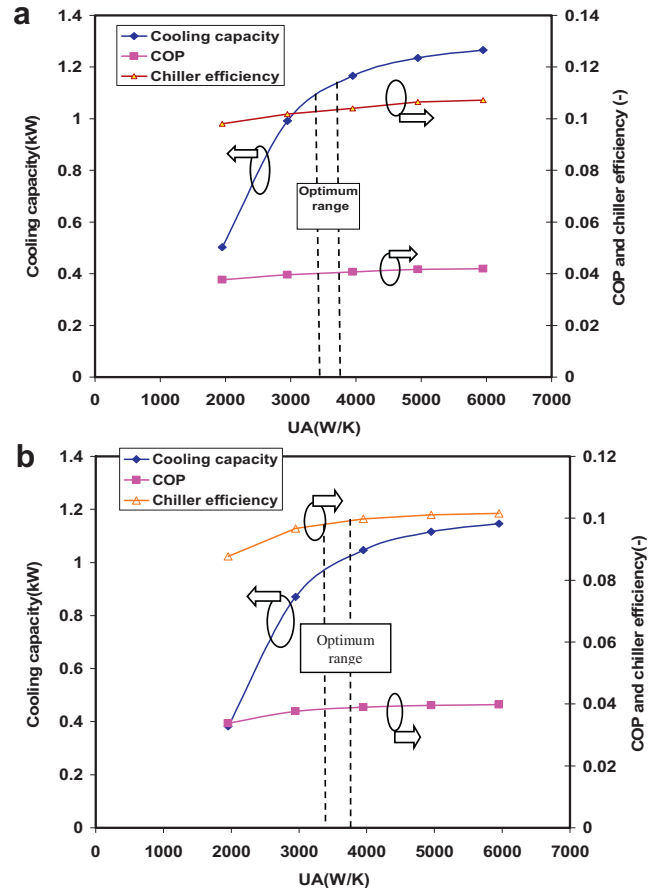
cooling capacity, COP and chiller efficiency for the combined cycle are shown in Fig. 4. As can be seen from Fig. 4 the cooling capacity increases with the increase of switching time up to 50 s and cooling capacity decreases for the switching time higher than 50 s. However, the COP and chiller efficiency increase moderately during the switching time between 5 and 55 s, after that the improvement in COP and chiller efficiency with switching time is only marginal. It is clear from Fig. 4 that the optimum values of COP and chiller efficiency are around 0.06 and 0.18, respectively when the switching time is between 45 and 50 s.

4.4. Size of beds

Fig. 5a and b depicts the combined effects of the heat exchanger sizes (A) of sorption elements (SE) and the overall heat transfer coefficient, U (due to heat transfer fluids, heat exchanger materials, type of assorted adsorbent and adsorbate pairs) of the SE on cooling capacity, COP and chiller
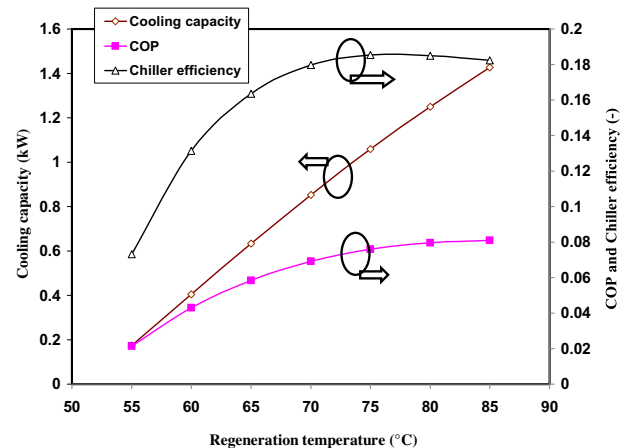

Fig. 5 − (a) Effect of UA values of R134a cycle on cooling capacity, COP and chiller efficiency. (b) Effect of UA values of R507A cycle on cooling capacity, COP and chiller efficiency.

efficiency, respectively for optimum cycle time, switching time and heat transfer fluid flow rates and the values are furnished in Table 2 for rated conditions. It can be seen that the cooling capacity increases with the increase of UA values

Fig. 4 − Effect of switching time on cooling capacity, COP and chiller efficiency for combined adsorption cycle.

Fig. 6 − Effect of regeneration temperature combined adsorption cycle on cooling capacity, COP and chiller efficiency.
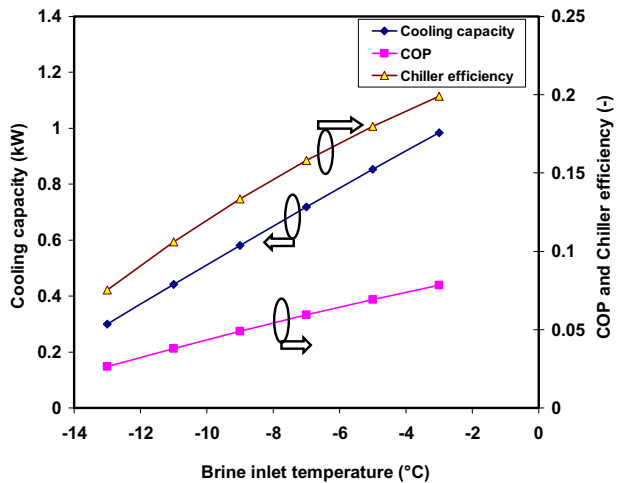
Fig. 7 – Brine inlet temperature effect on cooling capacity, COP and chiller efficiency for combined adsorption cycle.

of both R134a and R507A based sorption elements. However, the COP and chiller efficiency increase moderately with the increase of UA values. It is clear from Fig. 5a that the optimum values of COP and chiller efficiency for R134a are around 0.04 and 0.10, respectively, whereas from Fig. 5b it is observed that the optimum values of COP and chiller efficiency for R507A cycle are around 0.037 and 0.099, respectively. For both the topping and bottoming cycles the UA values vary from 3500 to 3800 W/K. From Table 3, it can be observed that the UA values for condenser of the topping cycle and evaporator of the bottoming cycle are 15,330 and 4770 W/K, respectively.

4.5. Regeneration temperature

Fig. 6 shows the effects of regeneration temperature on cooling capacity, COP and chiller efficiency with fixed cooling water and brine inlet temperatures. Heat transfer fluid flow rates and cycle times are taken as the rated values which are shown in Table 2. It can be seen from Fig. 6 that the cooling capacity increases linearly from 0.17 to 1.4 kW; with heat source temperatures varies from 55 to 85 °C. This is due to the amount of refrigerant circulation increases when the amount of desorbed refrigerant increases with the higher driving heat source temperature. The simulated COP and chiller efficiency values of combined cycle as shown in Fig. 6 increase with the rise of regeneration temperature until 70 °C. After that the increase of COP and chiller efficiency with regeneration temperature becomes marginal.

4.6. Brine inlet temperature

The effects of brine inlet temperature on cooling capacity, COP and chiller efficiency for the combined cycle are shown in Fig. 7. It is observable from Fig. 7 that the cooling capacity, COP and chiller efficiency of combined cycle increase with the increase of brine inlet temperature.

5. Conclusions

Based on a cycle simulation model, the paper presents the performance data of combined adsorption refrigeration cycles with AC-R134a in the upper and AC-R507A in the lower stages. An integrated evaporator–condenser heat exchanger is used in which the evaporator of R134a cycle cools the condenser of R507A cycle and there is no mass transfer between them. Simulation results show that when the cycle and switching times increase, both the COP and chiller efficiency increase, but the rate of increase diminishes at relatively higher cycle and switching times. This novel combined cycle can generate refrigeration at −10 °C with heat source temperature of 70 °C, which can be useful for freezing applications. Moreover, the combined systems could be significantly beneficial in process industries where a large amount of waste heat is available and reduction of greenhouse gas emissions is a major criterion.

REFERENCES

Alam, K.C.A., 2000. Design aspects of adsorption refrigeration systems. Ph.D. thesis, Tokyo University of Agriculture and Technology, Japan.

Anyanwu, E.E., Ezekwe, C.I., 2003. Design, construction and test run of a solid adsorption solar refrigerator using activated carbon/methanol as adsorbent/adsorbate pair. Energy Convers. Manage. 44 (18), 2879–2892.

Banker, N.D., Dutta, P., Prasad, M., Srinivasan, K., 2008. Performance studies on mechanical + adsorption hybrid compression refrigeration cycles with HFC-134a. Int. J. Refrigeration 31 (8), 1398–1406.

Chinnappa, J.C.V., Crees, M.R., Murthy, S.S., Srinivasan, K., 1993. Solar-assisted vapor compression/absorption cascaded air-conditioning systems. Sol. Energ. 50 (5), 453–458.

Chua, H.T., Ng, K.C., Wang, W., Yap, C., Wang, X.L., 2004. Transient modeling of a two-bed silica gel-water adsorption chiller. Int. J. Heat Mass Transf. 47 (4), 659–669.

Dawoud, B., 2007. A hybrid solar-assisted adsorption-cooling unit for vaccine storage. Renew. Energ. 32 (6), 947–964.

Douss, N., Meunier, F., 1989. Experimental study of cascaded adsorption cycles. Chem. Eng. Sci. 44 (2), 225–235.

El-Sharkawy, I.I., Kuwahara, K., Saha, B.B., Koyama, S., Ng, K.C., 2006. Experimental investigation of activated carbon fiber/ethanol pairs for adsorption cooling system application. Appl. Therm. Eng. 26 (8–9), 859–865.

El-Sharkawy, I.I., Saha, B.B., Koyama, S., Srinivasan, K., 2007. Isosteric heats of adsorption extracted from experiments of ethanol and HFC-134a on carbon based adsorbents. Int. J. Heat Mass Transf. 50 (5–6), 902–907.

Habib, K., 2009. Study on Activated Carbon Based Adsorption Refrigeration Cycles. Ph.D. thesis, Kyushu University, Japan.

Habib, K., Saha, B.B., Rahman, K.A., Chakraborty, A., Koyama, S., Ng, K.C., 2010. Experimental study of adsorption kinetics of activated carbon/R134a and activated carbon/R507A pairs. Int. J. Refrigeration 33 (4), 706–713.

Hirota, Y., Sugiyama, Y., Kubota, M., Watanabe, F., Kobayashi, N., Hasatani, M., Kanamori, M., 2008. Development of a suction-pump-assisted thermal and electrical hybrid adsorption heat pump. Appl. Therm. Eng. 28 (13), 1687–1693.

Lai, H.M., 2000. An enhanced adsorption cycle operated by periodic reversal forced convection. Appl. Therm. Eng. 20 (7), 595–617.

Liu, Y., Leong, K.C., 2006. Numerical study of a novel cascading adsorption cycle. Int. J. Refrig. 29 (2), 250–259.

Meunier, F., 1986. Theoretical performances of solid adsorbent cascading cycles using the zeolite-water and active carbon-methanol pairs: four case studies. Heat Recovery Syst. 6 (6), 491–498.

Meunier, F., 1998. Solid sorption heat powered cycles for cooling and heat pumping applications. Appl. Therm. Eng. 18 (9–10), 715–729.

Miles, D.J., Shelton, S.V., 1996. Design and testing of a solid-sorption heat pump system. Appl. Therm. Eng. 16 (5), 389–394.

Pons, M., Guilleminot, J.J., 1986. Design of an experimental solar powered, solid adsorption ice maker. J. Sol. Energ. Eng. (Trans. ASME) 103 (4), 332–337.

Saha, B.B., 1997. Performance Analysis of Advanced Adsorption Cycle. Ph.D. thesis, Tokyo University of Agriculture and Technology, Japan.

Saha, B.B., Akisawa, A., Kashiwagi, T., 2001. Solar/waste heat driven two-stage adsorption chiller: the prototype. Renew. Energ. 23 (1), 93–101.

Saha, B.B., Koyama, S., Lee, J.B., Kuwahara, K., Alam, K.C.A., Hamamoto, Y., Akisawa, A., Kashiwagi, T., 2003. Performance evaluation of a low-temperature waste heat driven multi-bed adsorption chiller. Int. J. Multiphas. Flow 29 (8), 1249–1263.

Saha, B.B., Chakraborty, A., Koyama, S., Ng, K.C., Sai, M.A., 2006. Performance modeling of an electro-adsorption chiller. Philos. Mag. Lett. 86 (23), 3613–3632.

Saha, B.B., El-Sharkawy, I.I., Chakraborty, A., Koyama, S., 2007a. Study on an activated carbon fiber-ethanol adsorption chiller: part I-system description and modeling. Int. J. Refrigeration 30 (1), 86–95.

Saha, B.B., El-Sharkawy, I.I., Chakraborty, A., Koyama, S., 2007b. Study on an activated carbon fiber-ethanol adsorption chiller: part II-performance evaluation. Int. J. Refrigeration 30 (1), 96–102.

Saha, B.B., El-Sharkawy, I.I., Habib, K., Koyama, S., Srinivasan, K., 2008. Adsorption of equal mass fraction near an azeotropic mixture of pentafluoroethane and 1,1,1-trifluoroethane on activated carbon. J. Chem. Eng. Data 53 (8), 1872–1876.

Saha, B.B., Habib, K., El-Sharkawy, I.I., Koyama, S., 2009. Adsorption characteristics and heat of adsorption measurements of R-134a on activated carbon. Int. J. Refrigeration 32 (7), 1563–1569.

Wang, D.C., Xia, Z.Z., Wu, J.Y., 2006. Design and performance prediction of a novel zeolite-water adsorption air conditioner. Energy Convers. Manage. 47 (5), 590–610.

Wang, R.Z., Jia, J.P., Zhu, Y.H., Teng, Y., Wu, J.Y., Cheng, J., Wang, Q.B., 1997. Study on a new solid adsorption refrigeration pair: activated carbon fiber-methanol pair. Trans. ASME 119, 214–218.

Zhang, L.Z., 2000. Design and testing of an automobile waste heat adsorption cooling system. Appl. Therm. Eng 20 (1), 103–114.